Desalination and Water Treatment
www.deswater.com
doi: 10.1080/19443994.2016.1186566

57 (2016) 27557–27572
December

Taylor & Francis
Taylor & Francis Group

Batik effluent reclamation through a task-orientated coupling process of nanofiltration membranes

Xiaojuan Wang[a,b], Xueli Gao[a,b,*], Yushan Zhang[c], Xinyan Wang[d], Congjie Gao[a,b]

[a]*Key Laboratory of Marine Chemistry Theory and Technology, Ministry of Education, Ocean University of China, Qingdao 266100, Shandong, China, Tel./Fax: +86 0532 66782017; emails: safiya0524@163.com (X. Wang), gxl_ouc@126.com (X. Gao), gaocjie@ouc.edu.cn (C. Gao)*
[b]*College of Chemistry and Chemical Engineering, Ocean University of China, Qingdao 266100 Shandong, China*
[c]*Institute of Tianjin Seawater Desalination and Multipurpose Utilization, State Oceanic Administration, Tianjin 300192, China, Tel./Fax: +86 022 87894686; email: dhskjc@vip.163.com*
[d]*Shandong Zhaojin Motian Co., Ltd, Zhaoyuan 265400, Shandong, China, Tel./Fax: +86 18660539881; email: zy_wxy@163.com*

Received 1 December 2015; Accepted 7 April 2016

ABSTRACT

Batik industries generate large amounts of effluents with high chromaticity, chemical oxygen demand (COD), turbidity, and salinity. The present study aims to recycle batik effluent using nanofiltration (NF) membranes. The effects of various operating conditions on the performances of three NF membranes (NF6, NF2A, and NF3A) were examined in terms of the removal rate of salt, COD, and chromaticity, together with permeate flux. Membrane fouling and cleaning strategies were also investigated. Results showed that the NF3A membrane outperformed the other membranes under the following optimal operating conditions: operating pressure, 1 MPa; operating temperature, 20°C; and cross-flow velocity, 5 m/s. A pilot-scale test was conducted by screening a NF membrane combination, including one NF membrane with high permeate fluxes and a poor water quality and another NF membrane placed on the opposite side, to satisfy reuse requirements and to reduce investment costs. Compared with NF3A membranes alone, the combination of NF2A and NF3A membranes could reduce COD and chromaticity to satisfy the reuse requirement and to enhance water fluxes. Through chemical cleaning with 3.5 ppm EDTA-2Na and 400 ppm NaOH, the performance of the NF membranes could be effectively restored. A feasible NF coupling process was confirmed in batik wastewater reclamation.

Keywords: Batik effluent; Reclamation; Nanofiltration; Coupling process; Membrane fouling and cleaning

1. Introduction

Batik printing technology has been extensively applied in local regions across China. With the rapidly growing demands for batik products, batik industries have proportionally increased. As a consequence, the amount of batik effluent discharged with high chromaticity, biochemical oxygen demand, chemical oxygen demand (COD), turbidity, salinity, and toxic chemicals has sharply increased in local areas [1–3]. Batik effluents cannot be discharged directly because it may pollute water bodies and disrupt ecological

*Corresponding author.

balance via the decreased photosynthetic activity of aquatic organisms [4,5]. Batik effluents also contain different organic contaminants, such as waxes, sizing agents, indigo dyes, and surfactants, which exhibit low biodegradability because of their complex structures and high molecular weights [6–8]. As such, batik effluent-related issues must be resolved.

Batik effluents are subjected to biochemical or physical–chemical treatments before they are discharged into municipal sewage [9]. In biochemical treatments, COD is efficiently removed; colors are also partially cleared without affecting salinity [10,11]. In physical–chemical treatments, dyes, suspended solids, and non-settleable materials are effectively removed from effluents [12]. In contrast to biochemical treatments, physical–chemical treatments are largely ineffective for the removal of soluble COD from effluents [9,13,14]. Advanced oxidation processes are costly and thus are not recommended for large-scale practical applications, although these processes provide positive effects on effluent treatments [15–20]. However, treatment methods exhibit unique advantages and disadvantages. Thus, the combination of these methods is generally used as appropriate.

Effluents have been recycled by water-intensive industries because of water scarcity and increasingly stringent regulations [21]. As such, advanced treatments should be applied to satisfy the requirements of batik effluents' reclamation and wastewater discharge reduction. For instance, membrane technology can be used in the reclamation of textile effluent to achieve a high treatment efficiency and enhanced quality of treated water [22–24]. Among pressure-driven membranes, nanofiltration (NF) membranes are efficient and essential for textile effluent reclamation [25–28]. NF membranes involve various separation mechanisms, including sieving effect and electrostatic effect, which can be efficient for the removal of organic compounds and salts [29,30]. In contrast to reverse osmosis membranes, NF membranes can be operated with low energy consumption and high selectivity and permeate flux [31,32]. Therefore, NF technology for textile effluent reclamation has been widely explored [33–37].

Batik technology is different from textile printing technology. In batik printing processes, waxes are used as resist agents to form printing patterns. After dyeing is completed, waxes should be washed and removed from materials. As a consequence, batik effluents contain abundant waxes, dewaxing agents, and various salts with extremely higher COD, chromaticity, and salinity than traditional textile printing effluents do. Thus far, batik effluent reclamation has been rarely reported. Traditional treatment methods cannot satisfy the requirements of batik effluent reclamation. In contrast to traditional treatment methods, NF technology can remove a majority of organic substances and reduce the salinity of effluents. Hence, batik effluent reclamation with NF membranes should be systematically investigated. However, fouling by contaminants deposited on membrane surfaces inevitably occurs during batik effluent treatment processes; as such, the permeate flux can be reduced and the removal rate of solutes may be affected over time [38–40]. Hence, feasible cleaning strategies should be selected for membrane regeneration.

In our study, three kinds of NF membranes with different performances, such as high water flux, high salt and organic compound removal rate, antifouling, and easy cleaning, were selected on the basis of our previous research [41–44] on batik effluent reclamation. Their operating parameters, namely: operating pressure, temperature, and cross-flow velocity, were optimized to enhance the quality of reused water in bench-scale tests. For long-term full-scale applications, feasible chemical cleaning methods were also investigated. On the basis of our experimental results, a pilot-scale test was performed by screening the optimal NF membrane combination, that is, two NF membranes as a unit, one with a high permeate flux and poor water quality, and another membrane was placed on the opposite side, to fulfill the requirements of water reuse and to enhance the water fluxes of the system. Through these methods, investment costs may also be reduced.

2. Materials and methods

2.1. Materials

The batik effluent used in this study was collected from Qingdao Phoenix Printing Dyeing Co., Ltd, in Qingdao, Shandong Province, China. The batik products of this company are sold to over 20 countries and regions in Africa and Europe, and the international market share of similar products is >30%. Hence, large volumes of batik effluent are generated by this factory. Effluent reclamation is necessary because Qingdao is a hydropenic tourism city. Batik effluent is the output of existing wastewater treatment involving wax recovery, flocculation, anaerobic reaction, aerobic reaction, and precipitation.

Hydrazine sulfate and hexamethylenetetramine were chosen to prepare the standard solution for turbidity measurement. Potassium dichromate and cobalt monosulfate heptahydrate were selected to prepare the standard solution for chromaticity measurement. Hydrochloric acid, sodium hydroxide, and EDTA-2Na were used as chemical cleaning agents. These chemicals

were of analytical grade and used without further purification. Deionized water with a resistivity of 18.2 MΩ was used as pure water.

2.2. Membranes

Ultrafiltration (UF) membranes are hollow fiber modules with a selective layer of polyvinylidene fluoride on non-woven fabrics. These membranes exhibit excellent antifouling performances. The UF membrane module was provided by Shandong Zhaojin Motian Co., Ltd, in Zhaoyuan, Shandong Province. NF membranes are commercial spiral-wound membranes provided by Zhejiang Mey Technology Co., Ltd, in Hangzhou, Zhejiang Province. The functional layer materials of the NF membranes are composed of polyamides on non-woven fabrics. The characteristics of UF and NF membranes are shown in Tables 1 and 2, respectively.

2.3. Bench-scale and pilot-scale apparatuses

The bench-scale apparatus is presented in Fig. 1. The hollow fiber UF membrane filter unit was used in the pretreatment. In this process, the effluent was separated into permeate and concentrate containing suspended solids and macromolecular substances. The NF membrane unit was equipped with a feed tank (25 L), a pressure vessel containing the membrane module, a circulation and pressurization pump with a security valve and two pressure gauges, a thermometer for temperature measurement in the circulation reservoir [45], an automatic circulating cooling device for temperature control, and a flow meter on the feed water pipe.

The pilot-scale apparatus is illustrated in Fig. 2. The effluent samples were initially pretreated using a submerged hollow fiber UF membrane module, and the filtered solution was placed in the NF feed tank. Then, the effluent was sifted with a cartridge filter and further treated with the NF system composed of a combination of two NF membranes.

2.4. Experimental procedure

In the bench-scale experiment, the batik effluent was pretreated using the UF membrane at room temperature (20˚C) and applied pressure of 0.1 MPa. Before NF filtration experiments were performed, flat NF membrane pieces were soaked in deionized water for 24 h at room temperature and then precompacted by filtering with deionized water at an applied pressure of 2.0 MPa until a constant flux was obtained. The batik effluent was then introduced to the feed tank, and the test was carried out. A full circulation mode was used during the experiments to maintain a constant concentration of the NF feed. In this mode, the concentrate and permeate were returned to the feed tank. The feed solute concentration slightly decreased during the process because some solutes were deposited onto the membrane surface or the pipeline wall. Therefore, an extra feed was included in the feed tank to minimize feed concentration changes [46].

The effects of applied pressure, temperature, and cross-flow velocity on the performances of different NF membranes were investigated. A pilot-scale test was conducted on the basis of the permeation flux and the removal rate of organics under the optimal operating conditions using different combinations of two NF membranes to fulfill water reuse requirements and to reduce investment costs.

2.5. Analytical methods and calculations

The permeate flux was defined as the amount of permeate produced per unit area of membrane surface per unit time:

$$F = \frac{\Delta V}{A \cdot \Delta t} \tag{1}$$

where F is the permeate flux (L m^{-2} h^{-1}), ΔV is the volume of product water (L), A is the effective area of membrane surface (m^2), and Δt is the penetration time (h).

The conductivity and pH of the samples were measured with a conductivity meter (DDS-307A, Leici, China) and a pH meter (DELTA320, Zhanyi, China), respectively. Salt rejection was calculated as follows:

$$R = \left(1 - \frac{k_p}{k_f}\right) \times 100\% \tag{2}$$

where k_f is the feed electrical conductivity (μs/cm) and k_p is the permeate electrical conductivity (μs/cm).

Turbidity was determined on the basis of absorbance using a UV-2450 UV–vis spectrophotometer (3-cm cell width), in accordance with the national standard method (GB13200–91) of China. Chromaticity was determined on the basis of absorbance using a UV-2450 UV–vis spectrophotometer (1-cm cell width) after the samples were sieved using a 0.45-μm filter. Turbidity rejections were calculated using Eq. (3). Chromaticity rejections were determined in terms of

Table 1
Characteristics of UF membranes

Membrane code	MWCO (Dal)	Effective membrane area (m^2)	Inner and outer diameters (mm)	Range of pH
UF3OB160	100,000	30	0.8/1.3	2–11

Table 2
Characteristics of the NF membranes

Membrane code	DIW permeability (L m^{-2} h^{-1})[a]	Surface charge[b]	NaCl rejection (%)[c]	$MgSO_4$ rejection (%)[c]	Roughness (nm)[d]	Effective membrane area (m^2)[b]
NF6	120.0	Negative	16.0	50.0	5.969	7.0
NF2A	71.8	Negative	30.0	99.0	4.086	7.0
NF3A	53.5	Negative	38.0	99.5	3.207	7.0

[a]The values were measured in the study under the condition: deionized water at 1.0 MPa and room temperature.
[b]Information was provided by the manufacturer.
[c]NF test condition: NaCl or $MgSO_4$ 2 g/L in water at 1.0 MPa and room temperature.
[d]The values were measured in the study using a NanoScope 3D multimode AFM controller (Veeco, USA).

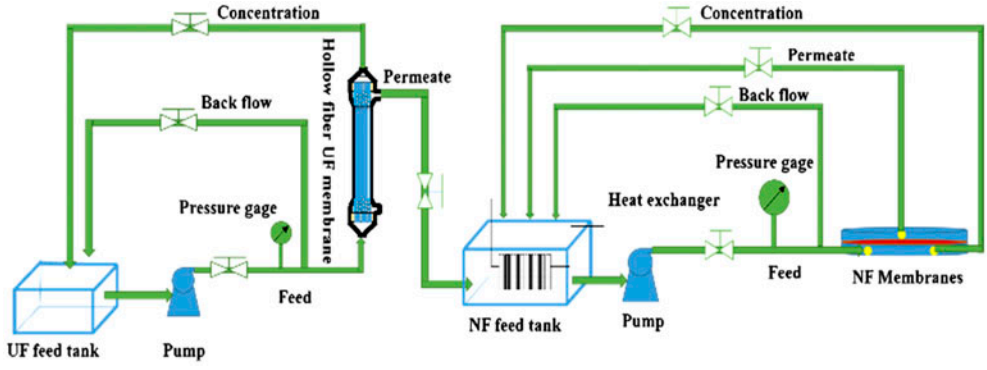

Fig. 1. Bench-scale apparatus used for batik effluent reclamation.

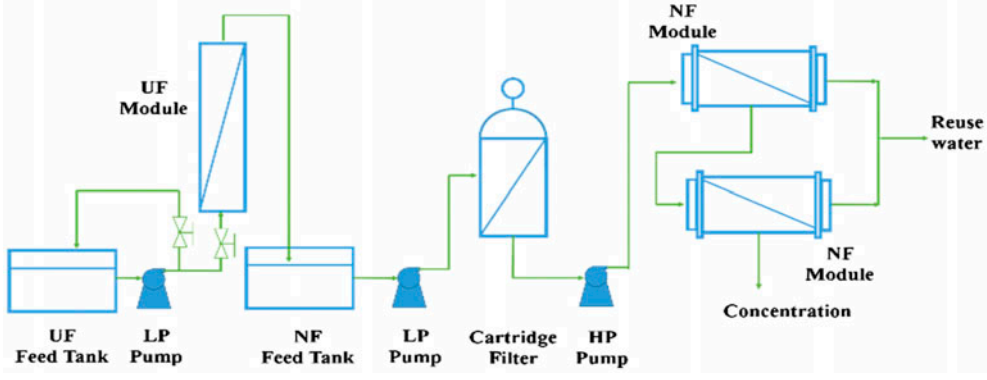

Fig. 2. Pilot-scale apparatus used for batik effluent reclamation.

the change in the ratio of absorbance to their maximum absorption wavelength:

$$R = \left(1 - \frac{T_p}{T_f}\right) \times 100\% \quad (3)$$

where T_f is the turbidity of the feed (NTU) and T_P is the turbidity of the permeate (NTU):

$$R = \left(1 - \frac{A_p}{A_f}\right) \times 100\% \quad (4)$$

where A_f is the feed absorbance and A_P is the permeate absorbance.

COD values were obtained using a HACH2005 direct reading spectrophotometer with a HACH COD reactor. COD removal was calculated using the following equation:

$$R = \left(1 - \frac{C_p}{C_f}\right) \times 100\% \quad (5)$$

where C_f is the feed COD value (mg/L) and C_p is the permeate COD value (mg/L).

2.6. Membrane fouling and cleaning

Membrane fouling occurs because of the deposition of dissolved organic and inorganic compounds on membrane surfaces. As a result, the permeate flux of NF membranes decreases gradually. In the pilot-scale test, water flux retention (WFR) was defined to characterize the antifouling property of different NF membrane combinations:

$$\mathrm{WFR}(\%) = \frac{J_{fw}}{J_{iw}} \times 100 \quad (6)$$

where J_{iw} is the pure water flux before fouling and J_{fw} is the pure water flux after fouling. Pure water fluxes were measured at an applied pressure of 1.0 MPa, cross-flow velocity of 5 m/s, and temperature of 20°C.

The membranes were chemically cleaned with HCl (pH 2, 365 ppm), NaOH (pH 12, 400 ppm), and EDTA-2Na (3.5 ppm) on flat-sheet bench-scale NF equipment (Section 2.3) to remove contaminants from the membrane surface. Fouled membranes, such as NF3A, were cleaned at 0.1 MPa, 5 m/s, and 20°C. Then, the cleaning effects were characterized by obtaining flux recovery ratio (FRR) and performing scanning electron microscopy (SEM) and atomic force microscopy (AFM). FRR was calculated in terms of the pure water flux measured in different circumstances [47,48]:

$$\mathrm{FRR}\ (\%) = \frac{J_w - J_{fw}}{J_{iw} - J_{fw}} \times 100 \quad (7)$$

where J_{iw} is the pure water flux before fouling, J_{fw} is the pure water flux after fouling, and J_w is the pure water flux after cleaning. Pure water fluxes were measured at 1.0 MPa, 5 m/s, and 20°C.

The samples were cut into desired sizes and coated with gold powder on the surface using a sputter coating machine prior to observation. The images of the initial, fouled, and chemically cleaned membranes were observed using an S-4800 scanning electron microscope (Hitachi High-Technologies Corporation, Japan) at a 7.0 kV accelerating voltage and a magnification of 10,000 times. AFM measurements were performed using a NanoScope 3D multimode AFM controller (Veeco, USA). Membrane samples were fixed onto the substrate and observed in a tapping mode. A resolution of 512 × 512 data points at 1 Hz per image was set to collect the images. A high-accuracy morphology diagram of the membrane surface could be achieved, and surface roughness was calculated using the built-in software.

3. Results and discussion

3.1. Pretreatment effects of UF membranes on batik effluent

UF membranes were used as a pretreatment to eliminate suspended solids and to clear batik effluent turbidity. The characteristics of feed water and UF effluent are shown in Table 3. The removal rates of turbidity, COD, and chromaticity are >99, 25, and 7%, respectively. The removal of water contaminants by the UF membrane mainly depends on the sieving effect. Thus, membrane pore size plays a decisive role in contaminant removal. The volume of compounds greater than the UF membrane pore size is retained in the inlet side of the membranes because the molecular weight cut-off (MWCO) of UF membranes is 100,000 Dalton. Moreover, the UF membrane with an uncharged surface and a large membrane pore size almost does not elicit a desalination effect. Therefore, UF membranes have achieved a better performance as pretreatment for subsequent NF processes.

Table 3
Water quality of feed water and UF effluent

Water quality	COD (mg/L)	Turbidity (NTU)	Conductivity (ms/cm)	Chromaticity (°)	pH
UF influent	448	302	11.63	841	8.38
UF effluent	338	2	11.18	779	8.14

3.2. Effects of operating conditions on the performances of the NF system

3.2.1. Effects of operating pressure

The effects of operating pressure on permeate flux and removal rates of COD, chromaticity, and salinity of the three NF membranes are described in Fig. 3.

Fig. 3(a) and (b) reveals that permeate flux and salt rejection are proportional to the applied pressure for all of the NF membranes. Moreover, the increasing efficiencies of permeate flux and salinity rejection through the NF3A membrane are greater than those of the other membranes within the investigated pressure range. In particular, the salinity rejections of the NF3A

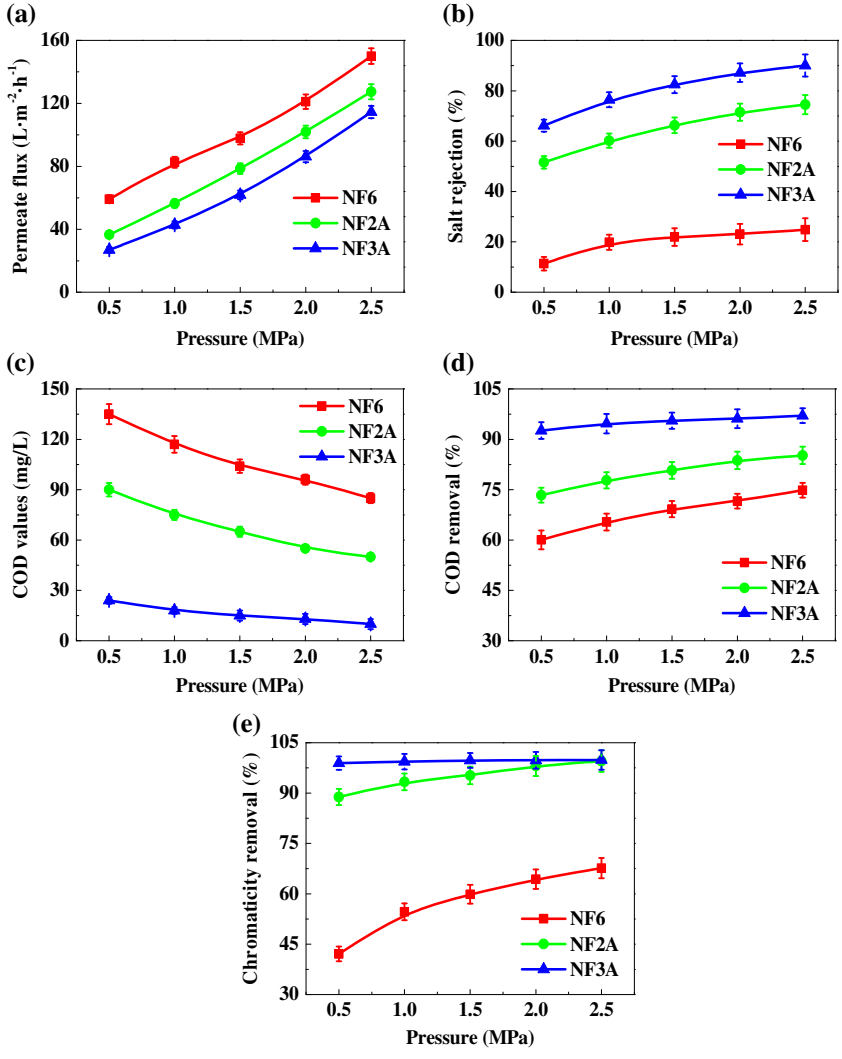

Fig. 3. Effects of applied pressure on (a) permeate flux and removal rates of (b) salinity, (c and d) COD, and (e) chromaticity of three NF membranes under constant conditions: temperature, 20°C; cross-flow velocity, 5 m/s.

membrane and the NF6 membrane are >66 and >11%, respectively.

Fig. 3(c) and (d) shows the increasing trend of the COD removal rate of the NF membranes as operating pressure increases. The COD removal rates of NF6, NF2A, and NF3A membranes are >60, >73, and 92%, respectively. In particular, the COD of the NF3A effluent is <25 mg/L, which is much lower than that of NF6 and NF2A effluents. This phenomenon can be accounted to the lower MWCO of the NF3A membrane than that of NF6 and NF2A membranes [43].

In Fig. 3(e), the chromaticity removal rates of the NF membranes are arranged in the following order: NF6 < NF2A < NF3A. This phenomenon occurs because the pore size of NF membranes is essential for the removal of organic compounds. This finding further illustrates the different pore size distributions of the three NF membranes. Moreover, the chromaticity removal rate of NF3A is not sensitive to changes in pressure.

An increase in operating pressure improves the driving pressure of NF membranes; as a result, water flux increases. The penetration amounts of salts and organic compounds almost remain unchanged. Hence, the rejections against salts, COD, and chromaticity increase as pressure increases. However, the optimal pressure should be 1 MPa because efficiency declines slowly when pressure is >1 MPa.

3.2.2. Effects of temperature

The effects of operating temperature on permeate flux, COD retention, chromaticity rejection, and salinity rejection of the three NF membranes are shown in Fig. 4.

The effects of temperature on permeate flux and salt rejection are shown in Fig. 4(a) and (b), respectively. The permeate flux increases significantly within the temperature range. However, the salinity rejection decreases slightly as temperature increases. In particular, the salinity rejection of the NF6 membrane is very low; by contrast, the salinity rejection of NF3A membrane is approximately 75%.

The COD removal efficiencies of the NF membranes at different operating temperatures and their corresponding COD values are shown in Fig. 4(c) and (d), respectively. The COD removal efficiency of the NF membranes reduces slightly as the operating temperature increases. The performances of the NF3A membrane are more stable than those of NF6 and NF2A membranes. The COD removal efficiency of the NF3A membrane is generally above 90%, and the COD value of the permeation is <25 mg/L.

Fig. 4(e) reveals that the chromaticity removal of NF membranes decreases linearly as temperature increases. The chromaticity removal rates of NF6 and NF2A membranes decrease slightly from 59 to 54% and from 95 to 91%, respectively. The chromaticity removal rate of the NF3A membrane is approximately 100%.

As temperature increases, the viscosity of liquids decreases and the activity of membrane polymer materials increases. Thus, water flux increases. Moreover, the diffusion rate of salts and organic compounds through the membrane accelerates because of temperature increase. As a result, the removal rates of salt, COD, and chromaticity decrease. Therefore, NF membrane systems should be operated at room temperature to reduce treatment costs and to satisfy water reclamation requirements.

3.2.3. Effects of cross-flow velocity

The effects of cross-flow velocity on the permeate flux and the removal rates of COD, chromaticity, and salinity of the three NF membranes are illustrated in Fig. 5.

The effects of cross-flow velocity on permeate flux and salt rejection are shown in Fig. 5(a) and (b), respectively. Permeate flux and salinity rejection increase gradually within the cross-flow velocity range.

Fig. 5(c) and (d) reveals the COD removal efficiency and the corresponding COD values of the NF membranes at different cross-flow velocities. The COD removal rates of the three NF membranes range from 64 to 70%, from 73 to 78%, and from 93 to 96%, respectively, when the cross-flow velocity increases from 2.5 to 10 m/s. Moreover, the COD value of the NF3A effluent is <25 mg/L. These results suggest that an appropriate cross-flow velocity is conducive to the decrease in COD values of batik effluent.

In Fig. 5(e), the respective chromaticity removal rates of NF6 and NF2A membranes increase significantly from 51 to 60% and from 90 to 96% as the cross-flow velocity changes. The chromaticity removal rate of the NF3A membrane is approximately 100% at each cross-flow velocity. The effluent appears transparent and colorless.

As cross-flow velocity increases, pressure increases and concentration polarization weakens. These changes increase the permeate flux and the rejection of salinity, COD, and chromaticity. In summary, the effects of cross-flow velocity on NF performances are much weaker than those of applied pressure. Thus, NF membrane systems should be operated at a low cross-flow velocity to satisfy water reclamation requirements and to reduce treatment costs.

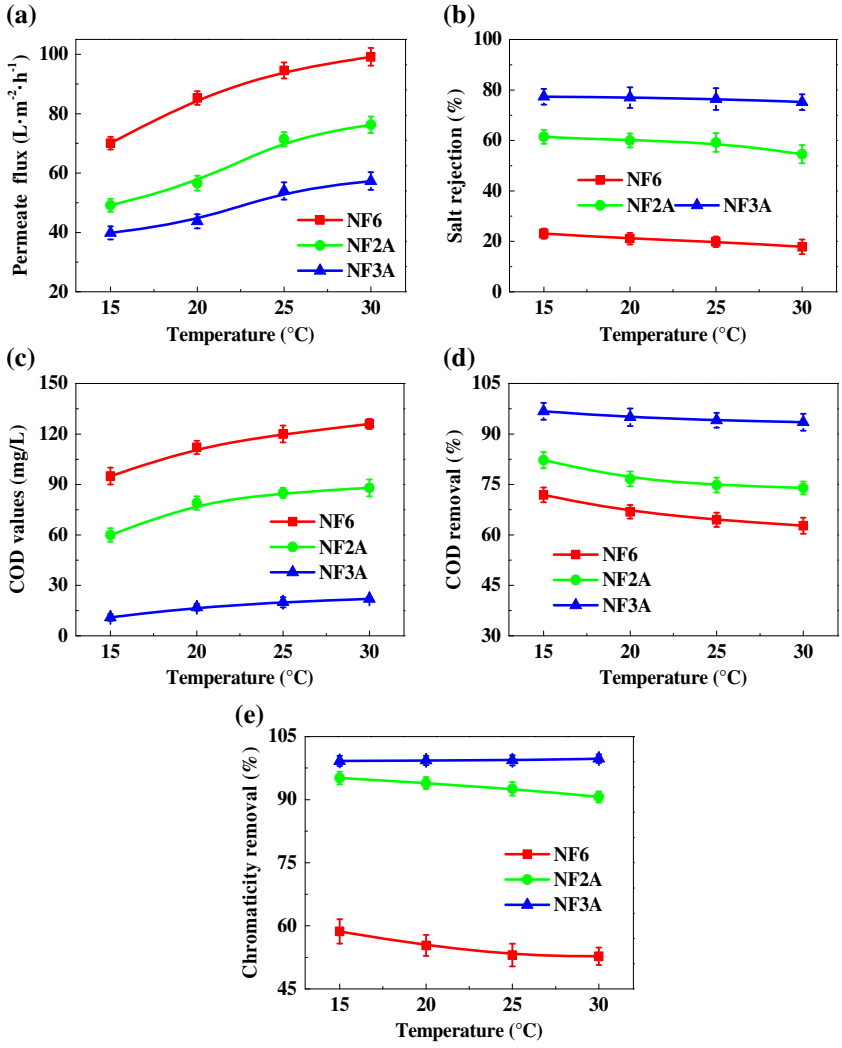

Fig. 4. Effects of applied temperature on (a) permeate flux and removal rates of (b) salinity, (c & d) COD, and (e) chromaticity of three NF membranes under constant conditions: pressure, 1.0 MPa; cross-flow velocity, 5 m/s.

Our results indicate that the optimum operating conditions of the NF membranes are as follows: operating pressure, 1 MPa; operating temperature, 20°C; and cross-flow velocity, 5 m/s. Table 4 summarizes the quality of the effluent water of the three NF membranes under the optimum conditions. The NF3A membrane can satisfy water reuse requirements, especially for COD and chromaticity. Conversely, the other NF membranes (NF6 and NF2A) are not effective for the removal of chromaticity and COD from batik effluent.

3.3. Pilot-scale tests to enhance treatment efficiency

The NF3A membrane is effective for the reclamation of batik effluent, whose COD and chromaticity values are much lower than the water reuse requirements. By comparison, NF6 and NF2A membranes do not satisfy the water reuse requirements in terms of COD and chromaticity values. Nevertheless, the permeate fluxes of NF6 and NF2A membranes are much higher than those of the NF3A membrane. Thus, different combinations of two NF membranes (NF6 + NF3A, NF2A + NF3A, and NF3A + NF3A) were used in the reclamation treatments for batik effluent in the pilot-scale tests under the optimum operating conditions to improve the water fluxes of the disposal system and to maintain the effluent quality that satisfies the water reuse requirements. The batik effluent was initially pretreated with submerged ultrafiltration membranes and further treated with NF membrane combinations. The water recovery of the UF membrane was 95% and backwash was conducted every half an hour. When the

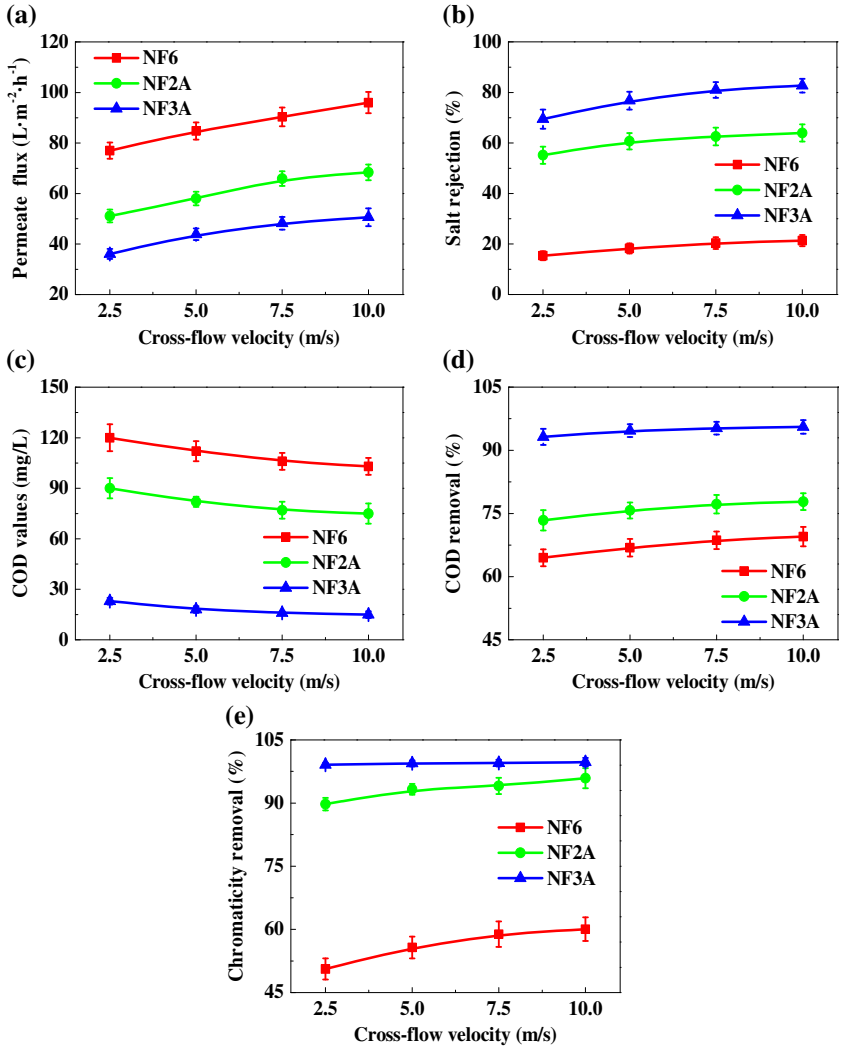

Fig. 5. Effects of cross-flow velocity on (a) permeate flux and removal rates of (b) salinity, (c & d) COD, and (e) chromaticity of three NF membranes under constant conditions: pressure, 1.0 MPa; temperature, 20℃.

Table 4
Quality of effluent water of the three NF membranes

Water quality	Permeate flux (L m^{-2} h^{-1})	Salinity removal (%)	COD (mg/L)	Chromaticity (°)
NF6	83	20	110	345
NF2A	56	60	80	50
NF3A	43	76	18	5
Reuse water	–	–	<50	<20

flux declined to 70% of the initial flux, chemical cleaning with cleanout fluid (acid wash: 1% citric acid solution; alkali wash: 0.5% sodium hydroxide solution +500 mg/L sodium hypochlorite solution) was carried out. The water recovery of the NF system was >85%, and batch filtering was performed in the experiment. The results are shown in Figs. 6 and 7.

The COD and color values of batik effluent and UF system permeate stream as a function of filtration time are presented in Fig. 6. The UF membrane used in this section can remove >25% of COD values and 7% of color values from the batik effluent. Moreover, >99% of turbidity is eliminated from the batik effluent. During the operating process, the COD value, the color

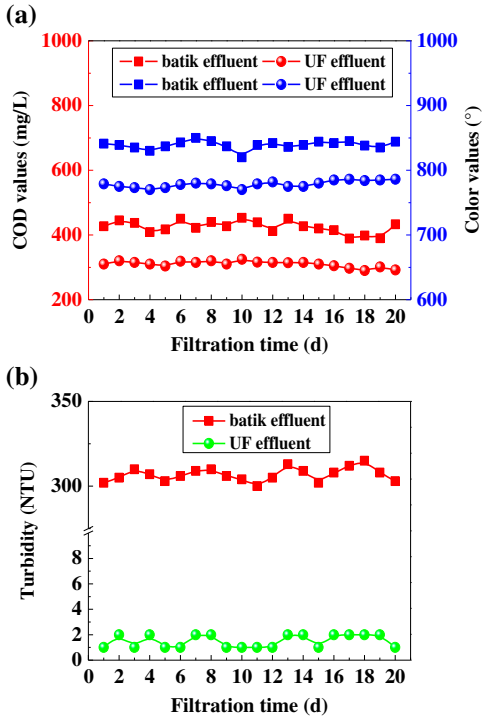

Fig. 6. Time-dependent COD values, color values, and turbidity of the batik effluent and the UF membrane permeate stream in the pilot-scale test.

value, and the turbidity of the UF membrane remain stable as the quality of batik effluent changes. Thus, the UF membrane plays a significant pretreatment role in subsequent NF filtration.

In Fig. 7(a), the water fluxes of the NF combinations decrease continuously with filtration time and gradually reach a steady state. The decline of water fluxes is mainly due to the deposition and adsorption of contaminants on membrane surfaces. Moreover, the permeate fluxes of two NF membrane combinations, namely, NF6 + NF3A and NF2A + NF3A, are much higher than those of the combination of two NF3A membranes in the operating period. In Section 3.2, the permeate fluxes of NF6, NF2A, and NF3A membranes are arranged as follows: NF6 > NF2A > NF3A. Under the same operating conditions, the permeate fluxes of the NF membrane combinations are as follows: (NF6 + NF3A) > (NF2A + NF3A) > (NF3A + NF3A). In particular, the water flux retention coefficiencies of NF6 + NF3A, NF2A + NF3A, and NF3A + NF3A membrane combinations are 69, 71, and 75%, respectively.

Fig. 7(b) and (c) depicts the COD and color values of the effluents of different NF membrane combinations with filtration time under the same operating conditions. The COD and color values of the NF2A and NF3A membrane combination are much lower

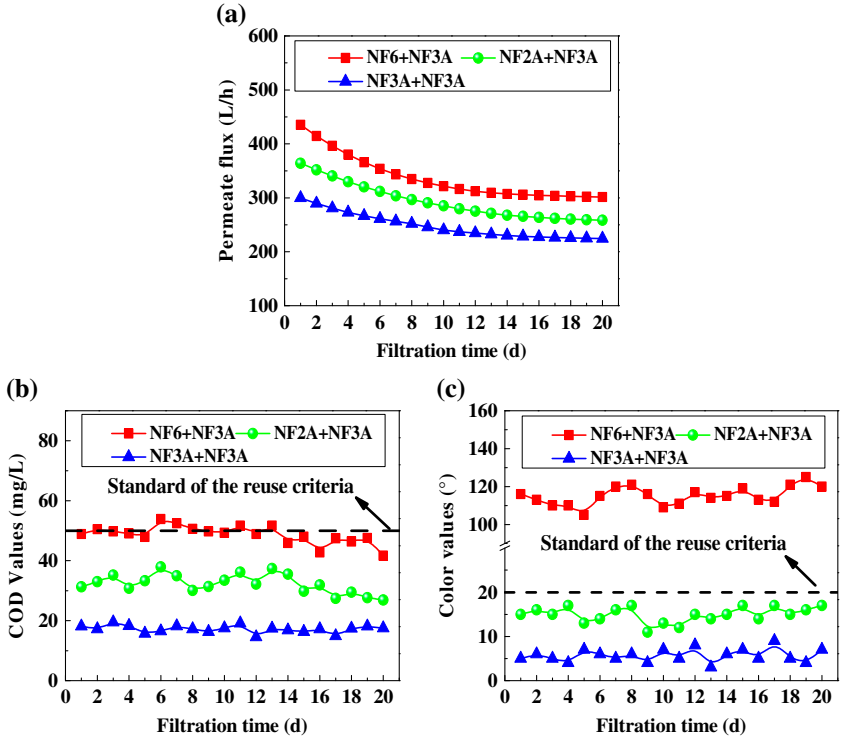

Fig. 7. (a) Permeate flux, (b) COD values, and (c) color values of different combinations of two NF membranes in the pilot-scale test under the following optimal conditions: pressure, 1.0 MPa; temperature, 20°C; and cross-flow velocity, 5 m/s.

than the water reuse requirement of the batik factory. For the NF6 and NF3A membrane combination, the COD values fluctuate within the water reuse criteria, but these values can be further reduced by enhancing the pretreatment effect of the UF system. The color values of the NF6 and NF3A membrane combination are higher than 100˚, which fail to satisfy the water reuse requirement (20˚). This phenomenon is due to the lower cross-linking rate of the NF6 membrane than that of the other membranes; as a result, the pore size of the NF6 membrane is larger than that of the other membranes. Hence, the removal effects of the NF6 membrane on color are much weaker than those of the other two NF membranes. The combination of NF6 and NF3A membranes fails to satisfy the reuse requirements of the batik factory, although the permeate flux of this combination is larger than that of the other combinations.

The combination of NF2A and NF3A membranes can eliminate COD and chromaticity values to fulfill the water reuse requirements and to enhance the permeate fluxes of the disposal system. In full-scale operating processes, enhancing water fluxes of the system means using less amount of NF membrane modules;

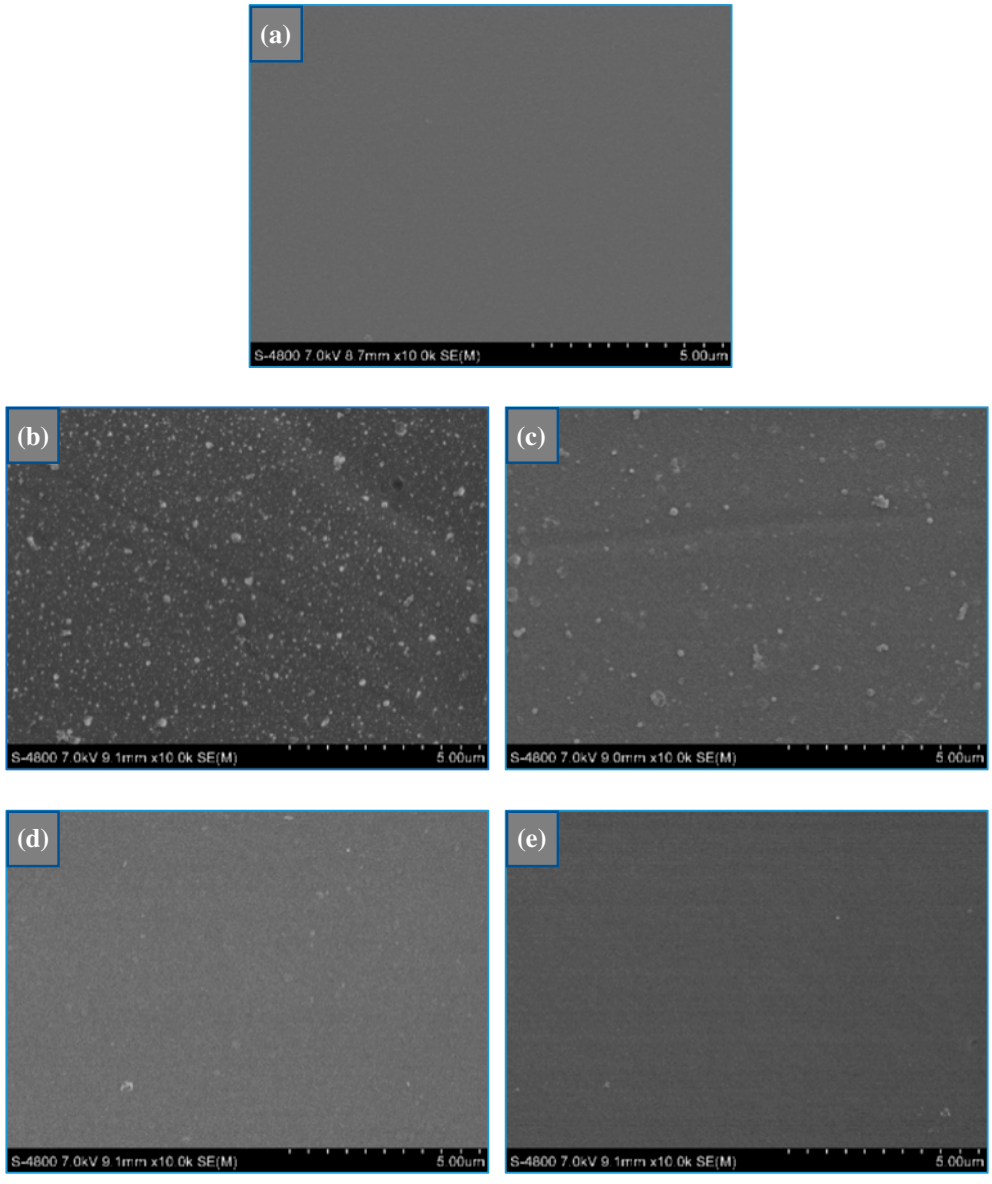

Fig. 8. SEM images of the surface morphologies of (a) original membrane, (b) fouled membrane, and membranes cleaned with, (c) HCl, (d) NaOH, and (e) EDTA-2Na.

as such, investment costs and covering area are reduced. In this way, Qingdao Phoenix Printing Dyeing Co., Ltd, could improve their effluent treatment system on the basis of our findings to reuse batik effluent in their production processes. The proposed system can effectively save freshwater and reduce pollution in the surrounding environment.

The volume of batik concentrate is less than 20% of the treated batik effluent. The concentration of the NF systems can be treated with advanced oxidation technologies or highly efficient evaporation methods [49–52]. However, treatment for the batik concentrate is beyond the scope of this work.

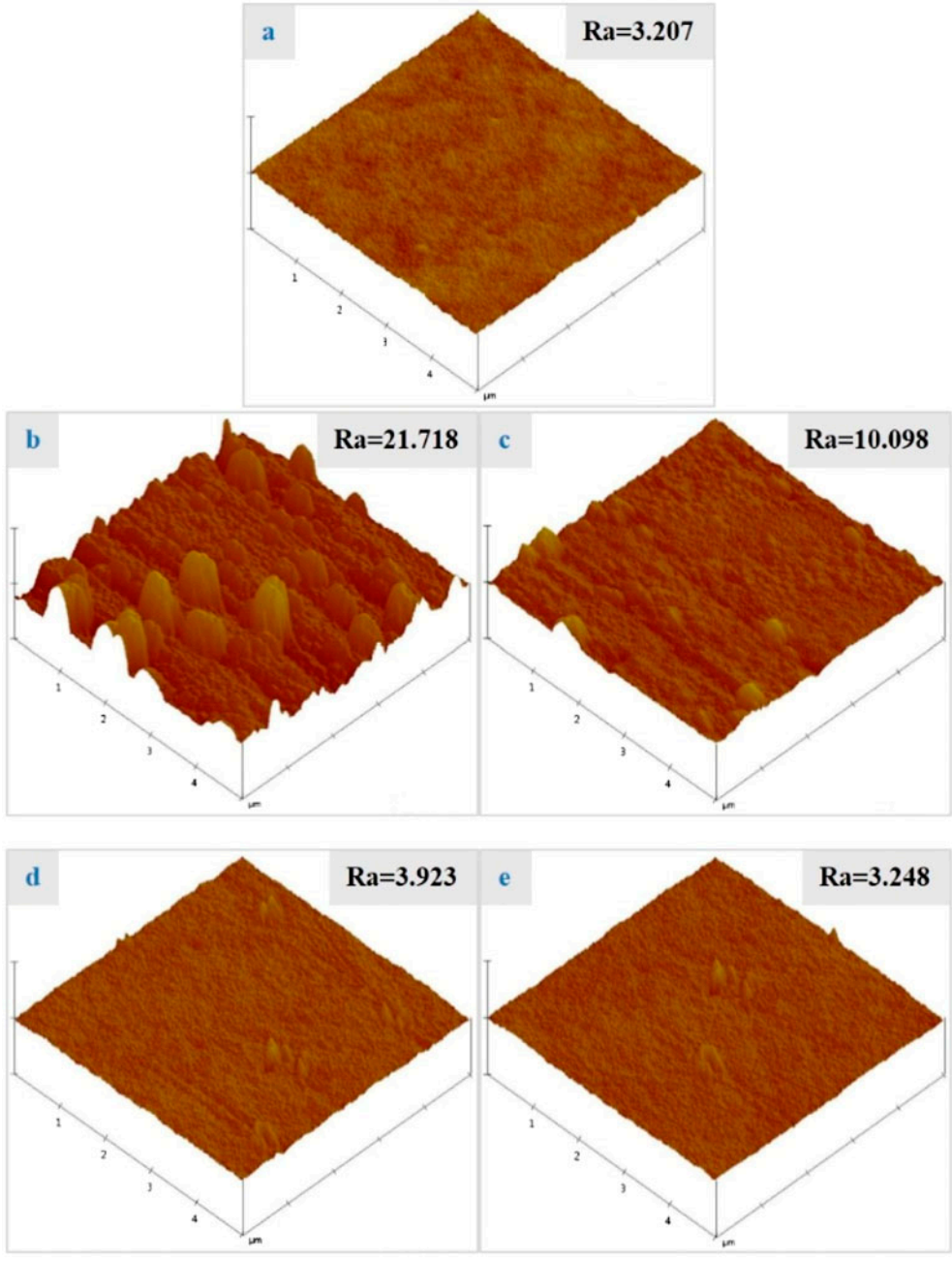

Fig. 9. AFM images of (a) original membrane, (b) fouled membrane, and membranes cleaned with, (c) HCl, (d) NaOH, and (e) EDTA-2Na.

3.4. Membrane chemical cleaning and regeneration

The cleaning efficiencies of the three methods were characterized through SEM (Fig. 8). The original membrane surface is smooth and neat. Many contaminants are adsorbed onto the fouled membrane surface. In Fig. 8, the membranes cleaned with NaOH and EDTA-2Na are quite similar to the original one. By contrast, HCl cleans a portion of the contaminants on the membrane surface. In Table 3, the contaminants on the NF membrane surface contain organic pollutants and inorganic salts. In contrast to NaOH and EDTA-2Na, HCl is ineffective for the removal of organic compounds.

The results of the chemical cleaning methods were examined through AFM, which is more visualized to evaluate their cleaning efficiencies. Three-dimensional stereograms and roughness are presented in Fig. 9. The original membrane surface is very smooth; by comparison, many peak valley structures are present on the fouled membrane surface. This finding implies that many pollutants are adsorbed onto the membrane surface. After the membrane surfaces were cleaned with HCl, NaOH, and EDTA-2Na, the surfaces become cleaner successively. The roughness of the original membrane is approximately 3.2 nm. The roughness of the polluted membrane is approximately 21.7 nm. The roughness values of the membranes cleaned with HCl, NaOH, and EDTA-2Na are 10.1, 3.9, and 3.2 nm, respectively. On the basis of these results, we found that the cleaning efficiencies of HCl are weaker than those of NaOH and EDTA-2Na.

A continuous operation test was conducted using the NF3A membranes for 72 h. After the test was completed, the contaminated membranes were cleaned with NaOH solution (pH 12), EDTA-2Na solution (3.5 ppm), and NaOH + EDTA-2Na solution (pH 12, 3.5 ppm). The cleaning efficiencies of different agents with respect to pure water flux recovery are presented in Fig. 10.

For the pollution formed during the long run operation, the cleaning effect of NaOH is the weakest among the three cleaning methods. This finding may be related to the fouling formation during the long run operation. Using NaOH, we experienced difficulty in achieving satisfactory results within a short time. However, EDTA-2Na is effective in dissolving organic matters and thus more conducive for cleaning fouled membranes. In addition, NaOH and EDTA-2Na elicit a synergistic effect; therefore, these agents are effective in recovering membrane permeate flux.

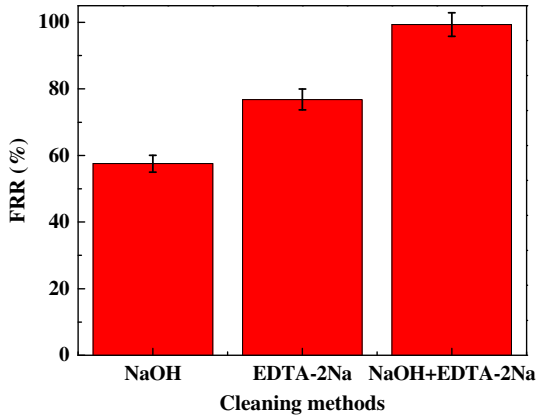

Fig. 10. FRR of NaOH and EDTA-2Na chemical cleaning for fouled membranes.

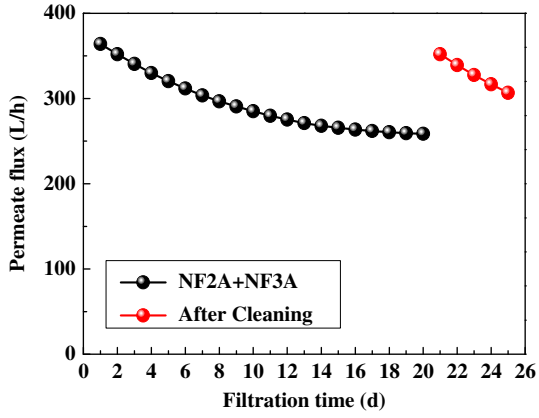

Fig. 11. Chemical cleaning effect on the NF2A and NF3A membrane combination in terms of permeate flux.

Hence, the synergistic use of NaOH and EDTA-2Na cleaning strategy is preferred during actual operation to restore membrane performance effectively.

Fig. 11 describes the time-dependent fluxes of the NF2A and NF3A membrane combination in the filtration of batik effluent subjected to the optimal conditions and cleaned with NaOH and EDTA-2Na. The water fluxes decrease continuously with filtration time and gradually reach constant values. The flux decline is mainly attributed to the deposition and adsorption of contaminants on the membrane surface. As such, chemical backwashing with the synergistic use of NaOH and EDTA-2Na was performed after the system was run for 20 d. The results reveal that the permeate flux after cleaning can be regenerated effectively.

4. Conclusion

The present investigation demonstrates a task-orientated coupling process of NF membranes for batik effluent reclamation. The NF membranes used in the bench-scale test can decrease the salinity, chromaticity, and COD of batik effluent to varying degrees. High operating pressure and cross-flow velocity are beneficial for permeate flux and water reuse quality. By contrast, high operating temperature elicits adverse effects on water reuse quality. The optimum operating conditions of all NF membranes are as follows: operating pressure, 1 MPa; operating temperature, 20˚C; and cross-flow velocity, 5 m/s. Under these conditions, the NF3A membrane is effective for the reclamation of batik effluent. Conversely, the effluent quality of NF6 and NF2A membranes fails to satisfy the water reuse requirements in terms of COD and chromaticity values. Nevertheless, the permeate fluxes of NF6 and NF2A membranes are much higher than those of the NF3A membrane. Considering these findings, we conducted a pilot-scale test using different combinations of two NF membranes, including one NF membrane with high permeate flux and poor water quality and the other placed on the opposite site to satisfy reuse requirements and to reduce investments costs. In contrast to the combination of two NF3A membranes, the combination of NF2A and NF3A membranes can eliminate COD and color values to fulfill the water reuse requirements and to enhance the water flux of the system. The combination of NF2A and NF3A membranes can also be applied to reduce investment costs. Chemical cleaning results also reveal that the synergistic effect of alkali and surfactant is more conducive for the recovery of the membrane properties during long-term operation.

Therefore, NF membranes can be utilized in the reclamation of batik effluent. The combination of two different NF membranes can also be used in other processes, such as drinking water purification and seawater desalination.

Acknowledgments

The authors gratefully acknowledge the financial support from the National Science and Technology Pillar Program during the 12th Five-year Plan Period (Grant nos. 2014BAK13B02 and 2015BAE06B03) and the Public Science and Technology Research Funds Projects of Ocean (Grant no. 201505021).

List of Symbols

F	—	permeate flux (L m^{-2} h^{-1})
R	—	rejection of salinity, COD, and chromaticity (%)
k_p	—	permeate electrical conductivity (μs/cm)
k_f	—	feed electrical conductivity (μs/cm)
A_p	—	permeate absorbance
A_f	—	feed absorbance
C_p	—	permeate COD value (mg/L)
C_f	—	feed COD value (mg/L)
T_f	—	turbidity of the feed (NTU)
T_p	—	turbidity of the permeate (NTU)
V	—	volume of product water (L)
A	—	effective area of membrane surface (m^2)
t	—	penetration time (h)
WFR	—	water flux retention (%)
FRR	—	flux recovery ratio (%)
J_w	—	pure water flux after cleaning (L m^{-2} h^{-1})
J_{fw}	—	pure water flux after fouling (L m^{-2} h^{-1})
J_{iw}	—	pure water flux before fouling (L m^{-2} h^{-1})

References

[1] A.K. Verma, R.R. Dash, P. Bhunia, A review on chemical coagulation/flocculation technologies for removal of colour from textile wastewaters, J. Environ. Manage. 93 (2012) 154–168.
[2] G. Tchobanoglous, F.L. Burton, Wastewater engineering, Management 7 (1991) 1–4.
[3] W. Lau, A.F. Ismail, Polymeric nanofiltration membranes for textile dye wastewater treatment: Preparation, performance evaluation, transport modelling, and fouling control—A review, Desalination 245 (2009) 321–348.
[4] L.A. de Luna, T.H. da Silva, R.F.P. Nogueira, F. Kummrow, G.A. Umbuzeiro, Aquatic toxicity of dyes before and after photo-Fenton treatment, J. Hazard. Mater. 276 (2014) 332–338.
[5] C. Kannan, K. Muthuraja, M.R. Devi, Hazardous dyes removal from aqueous solution over mesoporous aluminophosphate with textural porosity by adsorption, J. Hazard. Mater. 244–245 (2013) 10–20.
[6] B. Gao, Q. Yue, Y. Wang, W. Zhou, Color removal from dye-containing wastewater by magnesium chloride, J. Environ. Manage. 82 (2007) 167–172.
[7] T. Kim, C. Park, J. Yang, S. Kim, Comparison of disperse and reactive dye removals by chemical coagulation and Fenton oxidation, J. Hazard. Mater. 112 (2004) 95–103.
[8] A. Pala, E. Tokat, Color removal from cotton textile industry wastewater in an activated sludge system with various additives, Water Res. 36 (2002) 2920–2925.
[9] A. Bes-Piá, A. Iborra-Clar, C. García-Figueruelo, S. Barredo-Damas, M.I. Alcaina-Miranda, J.A. Mendoza-Roca, M.I. Iborra-Clar, Comparison of three NF membranes for the reuse of secondary textile effluents, Desalination 241 (2009) 1–7.

[10] A. Bes-Piá, M.I. Iborra-Clar, A. Iborra-Clar, J.A. Mendoza-Roca, B. Cuartas-Uribe, M.I. Alcaina-Miranda, Nanofiltration of textile industry wastewater using a physicochemical process as a pre-treatment, Desalination 178 (2005) 343–349.
[11] B. Guieysse, Z.N. Norvill, Sequential chemical-biological processes for the treatment of industrial wastewaters: Review of recent progresses and critical assessment, J. Hazard. Mater. 267 (2014) 142–152.
[12] I. Khouni, B. Marrot, P. Moulin, R.B. Amar, Decolourization of the reconstituted textile effluent by different process treatments: Enzymatic catalysis, coagulation/flocculation and nanofiltration processes, Desalination 268 (2011) 27–37.
[13] Y. Anjaneyulu, N.S. Chary, D.S.S. Raj, Decolourization of industrial effluents—Available methods and emerging technologies—A review, Rev. Environ. Sci. Biotechnol. 4 (2005) 245–273.
[14] F.I. Hai, K. Yamamoto, K. Fukushi, Hybrid treatment systems for dye wastewater, Crit. Rev. Environ. Sci. Technol. 37 (2007) 315–377.
[15] C.A. Basha, J. Sendhil, K.V. Selvakumar, P. Muniswaran, C.W. Lee, Electrochemical degradation of textile dyeing industry effluent in batch and flow reactor systems, Desalination 285 (2012) 188–197.
[16] Y. Yao, C. Zhao, M. Zhao, X. Wang, Electrocatalytic degradation of methylene blue on PbO_2-ZrO_2 nanocomposite electrodes prepared by pulse electrodeposition, J. Hazard. Mater. 263 (2013) 726–734.
[17] B. Haspulat, A. Gülce, H. Gülce, Efficient photocatalytic decolorization of some textile dyes using Fe ions doped polyaniline film on ITO coated glass substrate, J. Hazard. Mater. 260 (2013) 518–526.
[18] X. Zhang, W. Dong, F. Sun, W. Yang, J. Dong, Degradation efficiency and mechanism of azo dye RR2 by a novel ozone aerated internal micro-electrolysis filter, J. Hazard. Mater. 276 (2014) 77–87.
[19] A. Vijayabalan, K. Selvam, B. Krishnakumar, M. Swaminathan, Photocatalytic degradation of Reactive Orange 4 by surface fluorinated TiO_2 Wackherr under UV-A light, Sep. Purif. Technol. 108 (2013) 51–56.
[20] K. Turhan, I. Durukan, S.A. Ozturkcan, Z. Turgut, Decolorization of textile basic dye in aqueous solution by ozone, Dyes Pigm. 92 (2012) 897–901.
[21] C. Allegre, M. Maisseu, F. Charbit, P. Moulin, Coagulation-flocculation-decantation of dye house effluents: Concentrated effluents, J. Hazard. Mater. 116 (2004) 57–64.
[22] Q. Chen, Y. Yang, M. Zhou, M. Liu, S. Yu, C. Gao, Comparative study on the treatment of raw and biologically treated textile effluents through submerged nanofiltration, J. Hazard. Mater. 284 (2015) 121–129.
[23] E. Kurt, D.Y. Koseoglu-Imer, N. Dizge, S. Chellam, I. Koyuncu, Pilot-scale evaluation of nanofiltration and reverse osmosis for process reuse of segregated textile dyewash wastewater, Desalination 302 (2012) 24–32.
[24] E. Alventosa-deLara, S. Barredo-Damas, M.I. Alcaina-Miranda, M.I. Iborra-Clar, Ultrafiltration technology with a ceramic membrane for reactive dye removal: Optimization of membrane performance, J. Hazard. Mater. 209–210 (2012) 492–500.
[25] I. Koyuncu, D. Topacik, Effects of operating conditions on the salt rejection of nanofiltration membranes in reactive dye/salt mixtures, Sep. Purif. Technol. 33 (2003) 283–294.
[26] A. Akbari, J.C. Remigy, P. Aptel, Treatment of textile dye effluent using a polyamide-based nanofiltration membrane, Chem. Eng. Process. 41 (2002) 601–609.
[27] S. Mondal, Methods of dye removal from dye house effluent—An overview, Environ. Eng. Sci. 25 (2008) 383–396.
[28] G. Capar, U. Yetis, L. Yilmaz, Membrane based strategies for the pre-treatment of acid dye bath wastewaters, J. Hazard. Mater. 135 (2006) 423–430.
[29] A.R. Verliefde, E.R. Cornelissen, S. Heijman, J. Verberk, G.L. Amy, B. Van der Bruggen, J.C. van Dijk, The role of electrostatic interactions on the rejection of organic solutes in aqueous solutions with nanofiltration, J. Membr. Sci. 322 (2008) 52–66.
[30] P.S. Zhong, N. Widjojo, T. Chung, M. Weber, C. Maletzko, Positively charged nanofiltration (NF) membranes via UV grafting on sulfonated polyphenylenesulfone (sPPSU) for effective removal of textile dyes from wastewater, J. Membr. Sci. 417–418 (2012) 52–60.
[31] B. Van der Bruggen, G. Cornelis, C. Vandecasteele, I. Devreese, Fouling of nanofiltration and ultrafiltration membranes applied for wastewater regeneration in the textile industry, Desalination 175 (2005) 111–119.
[32] S.K. Nataraj, K.M. Hosamani, T.M. Aminabhavi, Distillery wastewater treatment by the membrane-based nanofiltration and reverse osmosis processes, Water Res. 40 (2006) 2349–2356.
[33] C.M. Nguyen, S. Bang, J. Cho, K. Kim, Performance and mechanism of arsenic removal from water by a nanofiltration membrane, Desalination 245 (2009) 82–94.
[34] A.Y. Zahrim, C. Tizaoui, N. Hilal, Coagulation with polymers for nanofiltration pre-treatment of highly concentrated dyes: A review, Desalination 266 (2011) 1–16.
[35] M. Liu, Z. Lü, Z. Chen, S. Yu, C. Gao, Comparison of reverse osmosis and nanofiltration membranes in the treatment of biologically treated textile effluent for water reuse, Desalination 281 (2011) 372–378.
[36] Y.K. Ong, F.Y. Li, S. Sun, B. Zhao, C. Liang, T. Chung, Nanofiltration hollow fiber membranes for textile wastewater treatment: Lab-scale and pilot-scale studies, Chem. Eng. Sci. 114 (2014) 51–57.
[37] S.R. Panda, S. De, Performance evaluation of two stage nanofiltration for treatment of textile effluent containing reactive dyes, J. Environ. Chem. Eng. 3 (2015) 1678–1690.
[38] M. Mondal, S. De, Treatment of textile plant effluent by hollow fiber nanofiltration membrane and multicomponent steady state modeling, Chem. Eng. J. 285 (2016) 304–318.
[39] N. Hilal, H. Al-Zoubi, N.A. Darwish, A.W. Mohammad, M.A. Arabi, A comprehensive review of nanofiltration membranes: Treatment, pretreatment, modelling, and atomic force microscopy, Desalination 170 (2004) 281–308.
[40] B. Van der Bruggen, M. Mänttäri, M. Nyström, Drawbacks of applying nanofiltration and how to avoid them: A review, Sep. Purif. Technol. 63 (2008) 251–263.
[41] L. Xu, X. Gao, Z. Li, C. Gao, Removal of fluoride by nature diatomite from high-fluorine water: An

appropriate pretreatment for nanofiltration process, Desalination 369 (2015) 97–104.
[42] W. Jiang, Y. Wei, X. Gao, C. Gao, Y. Wang, An innovative backwash cleaning technique for NF membrane in groundwater desalination: Fouling reversibility and cleaning without chemical detergent, Desalination 359 (2015) 26–36.
[43] W. Jiang, X. Gao, L. Xu, J. Wang, Investigation of synchronous arsenic and salinity rejection via nanofiltration system and membrane cleaning, Desalin. Water Treat. 57 (2016) 6554–6565.
[44] J. Wang, X. Gao, Y. Xu, Q. Wang, Y. Zhang, X. Wang, C. Gao, Ultrasonic-assisted acid cleaning of nanofiltration membranes fouled by inorganic scales in arsenic-rich brackish water, Desalination 377 (2016) 172–177.
[45] L. Braeken, B. Van der Bruggen, C. Vandecasteele, Flux decline in nanofiltration due to adsorption of dissolved organic compounds: Model prediction of time dependency, J. Phys. Chem. B 110 (2006) 2957–2962.
[46] Y. Yu, C. Zhao, Y. Wang, W. Fan, Z. Luan, Effects of ion concentration and natural organic matter on arsenic(V) removal by nanofiltration under different transmembrane pressures, J. Environ. Sci. 25 (2013) 302–307.
[47] X. Wei, Z. Wang, F. Fan, J. Wang, S. Wang, Advanced treatment of a complex pharmaceutical wastewater by nanofiltration: Membrane foulant identification and cleaning, Desalination 251 (2010) 167–175.
[48] S.S. Madaeni, Y. Mansourpanah, Chemical cleaning of reverse osmosis membranes fouled by whey, Desalination 161 (2004) 13–24.
[49] K. Praneeth, D. Manjunath, S.K. Bhargava, J. Tardio, S. Sridhar, Economical treatment of reverse osmosis reject of textile industry effluent by electrodialysis-evaporation integrated process, Desalination 333 (2014) 82–91.
[50] H. Guo, K. Jeong, J. Lim, J. Jo, Y.M. Kim, J. Park, J.H. Kim, K.H. Cho, Prediction of effluent concentration in a wastewater treatment plant using machine learning models, J. Environ. Sci. 32 (2015) 90–101.
[51] Y. Ren, Y. Yuan, B. Lai, Y. Zhou, J. Wang, Treatment of reverse osmosis (RO) concentrate by the combined Fe/Cu/air and Fenton process (1stFe/Cu/air-Fenton-2ndFe/Cu/air), J. Hazard. Mater. 302 (2016) 36–44.
[52] L. Zheng, X. Wang, X. Wang, Reuse of reverse osmosis concentrate in textile and dyeing industry by combined process of persulfate oxidation and lime-soda softening, J. Cleaner Prod. 108 (2015) 525–533.